RSC Advances

ROYAL SOCIETY OF CHEMISTRY

www.rsc.org/advances

Thermoelectric properties of $Fe_2MnSi_xGe_{1-x}$: Influence of vary Germanium content

A. H. Reshak[1,2*]

[1]*New Technologies - Research Centre, University of West Bohemia, Univerzitni 8, 306 14 Pilsen, Czech republic*

[2] *Center of Excellence Geopolymer and Green Technology, School of Material Engineering,*

Abstract

The semi-classical Boltzmann theory as implemented in the BoltzTraP code was used to study the influence of vary the germanium content on the thermoelectric properties of the Heusler compounds Fe_2MnSi and Fe_2MnGe. The electrical conductivity (σ / τ), Seebeck coefficient (S), the electronic power factor ($S^2\sigma$), electronic thermal conductivity (κ_e), electronic heat capacity $c_{el}(T_{el})$ and Hall coefficient (R_H), as a function of temperature at certain value of chemical potential (μ) with constant relaxation time (τ), were evaluated on the base of the calculated band structure using the standard Boltzmann kinetic transport theory and the rigid band approach. The increase/reduce in the electrical conductivity ($\sigma = ne\mu$) of $Fe_2MnSi_xGe_{1-x}$ alloys is attributed to the density of charge carriers (n) and their mobility ($\mu = e\tau/m_e$). The S for Fe_2MnGe is negative over the entire temperature range, which represents the n-type concentration. Whereas Fe_2MnSi show positive S up to 250 K then drop to negative values, which confirm the existence of the p-type concentration between 100-250 K. $Fe_2MnSi_{0.25}Ge_{0.75}$ / $Fe_2MnSi_{0.5}Ge_{0.5}$ / $Fe_2MnSi_{0.75}Ge_{0.25}$ possess positive S till 270 / 230 / 320 K then drop to negative values. The power factor of Fe_2MnGe rapidly increases with increasing the temperature, while for Fe_2MnSi it is zero till 300 K then rapidly increases with increasing the temperature. The $S^2\sigma$ of $Fe_2MnSi_{0.25}Ge_{0.75}$ have zero value between 250-350 K. Whereas $Fe_2MnSi_{0.5}Ge_{0.5}$ possess zero $S^2\sigma$ up to 320 K. The $Fe_2MnSi_{0.75}Ge_{0.25}$ have zero $S^2\sigma$ between 200-500 K. The electronic thermal conductivity (κ_e) and the electronic heat capacity $c_{el}(T_{el})$ increases with increasing the temperature. The parents compounds (Fe_2MnGe and Fe_2MnSi) show the highest positive value of Hall coefficient R_H at 100 K then drop to the negative values at 260 K. On the other hand the R_H for $Fe_2MnSi_{0.25}Ge_{0.75}$, $Fe_2MnSi_{0.5}Ge_{0.5}$ and $Fe_2MnSi_{0.75}Ge_{0.25}$ alloys exhibits negative R_H along the temperature scale. The behavior of R_H is attributed to the concentration of the charge carrier and their mobility.

Keywords:; *$Fe_2MnSi_xGe_{1-x}$; Heusler compounds; Thermoelectric properties; Power factor; Seebeck coefficient; electronic thermal conductivity*
[*]Corresponding author: *Reshak AH*
Tel. +420 777 729 583, *E-mail address:maalidph@yahoo.co.uk*

1. Introduction

Half metallic compounds has received a great deal of attention [1-13] due to the spin degree of freedom in electronics [14-17]. A strong effort has been paid to understanding the mechanism behind the half-metallic magnetism and to study its implication on various physical properties [18,19]. The field of spin based electronic (spintronics) has exploited a large class of emerging materials, such as ferromagnetic semiconductors [20, 21], high temperature superconductors [22], organic ferromagnets [23, 24], organic semiconductors [25], and carbon nanotubes [26, 27] based devices to bring novel functionalities to the traditional devices. In other areas within spintronics as high as possible a degree of spin polarisation is required, the half metals are considered the best. The half metallic compounds behave as metal for one spin direction, and behave as semiconductor or insulator for the opposite spin direction.

In 1983, de Groot et al. [28,29] discovered the half-metallic ferromagnetic (HMF). Even since this discovery, extensive studies are done and a lot of HMF have been theoretically predicted, then some of them were experimentally confirmed [30-32]. It is well known that the most important candidates for 100 % spin polarization are semi-Heusler alloys [19,28,29,33-35], zinc-blende structure materials [36, 37], semi-metallic magnetic oxides CrO_2 and Fe_3O_4 [11, 38,39] and full Heusler alloys [9, 40]. The $Fe_2MnSi_{1-x}Ge_x$ alloys are considered as very interested HMF materials [41-43]. The $Fe_2MnSi_{1-x}Ge_x$ alloys can be successfully applied to highly efficient spin injection and detection through Schottky tunnel barriers in group-IV semiconductor devices.

The epitaxial Fe_2MnSi thin films have a Curie temperature of about 210 K, which is much lower than room temperature [44], however, there is a limited experimental work. Zhang et al., have studied $Fe_2MnSi_{1-x}Ge_x$ alloys and found there is insignificantly change in the Curie temperature and the spontaneous magnetization, with change the Ge content in the single-phase $L2_1$ compounds. There is no field-induced transition and the magnetocaloric effect is rather small throughout the $Fe_2MnSi_{1-x}Ge_x$ series [45]. In addition, in the $L2_1$-type of structure, both Fe_2MnGe and Fe_2MnSi have a Curie temperature around 250 K [45]. Therefore, we thought it would be worthwhile to study the transport properties of the $Fe_2MnSi_xGe_{1-x}$ alloys by vary the germanium content between 0.0 and 1.0 with step of 0.25.

The rest of the paper is organized as; the structural aspects and the computational details are presented in section 2. The results and discussion are demonstrated in section 3. Section 4 summarize the results.

2. Structural aspects and computational Details

To study the influence of vary the germanium content on the thermoelectric properties of the Heusler compounds Fe_2MnSi and Fe_2MnGe, the semi-classical Boltzmann theory as implemented in the BoltzTraP code [46] was used. The thermoelectric transport tensors can be evaluated on the base of calculated band structure using the standard Boltzmann kinetic transport theory and the rigid band approach [47]. The electrical conductivity $\sigma_{\alpha\beta}$, Seebeck coefficient $S_{\alpha\beta}$ and electronic thermal conductivity $k^0_{\alpha\beta}$ tensors are the main transport properties.

In this work the germanium content in $Fe_2MnSi_xGe_{1-x}$ alloys was vary between 0.0 and 1.0 with step of 0.25. The parents compounds crystallize in $L2_1$ structure which consists of four face centered cubic sublattices with space Fm3m. The $L2_1$ phase is a cubic superstructure of four interpenetrating fcc sublattices, *A*, *B*, *C*, and *D*, centred at (0 0 0), (¼ ¼ ¼), (½ ½ ½) and (¾ ¾ ¾). Each *A* atom is at the centre of a cube of four *B* atoms and four *D* atoms (Fig.1). To trace the variation in the composition, we employ supercell approach. The electronic structure is calculated using the full potential linear augmented plane wave plus local orbitals method as implemented in WIEN2k code [48] with the Engel-Vosko generalized gradient approximation for the exchange correlation potential. The structures are fully relaxed by minimizing the forces acting on each atom. A mesh of 5000 ***k***-points in the irreducible Brillouin zone (IBZ) for binary as well as ternary alloys was used for calculating the thermoelectric properties. The K_{max} was set to be $9.0/R_{MT}$ and make the expansion up to l = 10 in the muffin tins spheres. The convergence of the total energy in the self-consistent calculations is taken with respect to the total charge of the system with a tolerance 0.0001 electron charges.

3. Results and discussion

3.1. Salient features of the electronic band structures

The calculated electronic band structure of $Fe_2MnSi_xGe_{1-x}$ (x=0.0, 0.25, 0.5, 0.75, 1.0) alloys along the high symmetry point in the first BZ were represented in Fig. 2 a-e. These figures suggest that the investigated alloys are metallic as it is clear that there exists some bands were controlled the overlapping around Fermi energy (E_F). The density of states at E_F is determined by the overlap between the valence and conduction bands. This overlap is strong enough indicating metallic origin with different values of DOS at E_F, $N(E_F)$ (Table I). The electronic specific heat coefficient (γ), which is function of density of states, can be calculated using the expression, $\gamma = \frac{1}{3}\pi^2 N(E_F)k_B^2$, where $N(E_F)$ is the density of states at E_F, and k_B is the Boltzmann constant. The calculated density of states at Fermi energy $N(E_F)$, enables us to calculate the bare electronic specific heat coefficient (Table I). It is clear that substituting 0.25 of Ge atoms by Si atoms led to increase the metallic nature of $Fe_2MnSi_{0.25}Ge_{0.75}$ by 3.7 % with respect to Fe_2MnGe, while substituting 0.5 of Ge atoms by Si atoms cause to increase the metallic nature of $Fe_2MnSi_{0.5}Ge_{0.5}$ by 1.9 % with respect to Fe_2MnGe. Further increasing the continent of Si atoms led to increase the metallic nature of $Fe_2MnSi_{0.75}Ge_{0.25}$ by 3.4 % with respect to Fe_2MnGe, finally substituting Ge by Si cause to reduce the metallic nature of Fe_2MnSi by 0.9 % with respect to Fe_2MnGe. The same trends was observed for the electronic specific heat coefficient (γ).

3.2. Transport properties

Fig. 3a, illustrated the influence of substituting of Ge by Si atom (with step of 0.25) on the electrical conductivity (σ/τ) of the Heusler compounds Fe_2MnGe and Fe_2MnSi. In all cases we notice that σ/τ increases with temperature, it is clear that the increasing rate is depend on the concentration of Ge and Si atoms. The end compounds (Fe_2MnGe and Fe_2MnSi) show the highest value for Fe_2MnSi of about $1.49\times10^{20}(\Omega ms)^{-1}$ at 100 K and $1.9\times10^{20}(\Omega ms)^{-1}$ at 800 K, while for Fe_2MnGe it is $1.4\times10^{20}(\Omega ms)^{-1}$ at 100 K and $1.82\times10^{20}(\Omega ms)^{-1}$ at 800 K. With substituting 0.25 of Ge by Si atom ($Fe_2MnSi_{0.25}Ge_{0.75}$) we noticed that the value of σ/τ drop to be the lowest values along the whole temperature range. Then after with increasing the content of Si atoms to be equal to Ge atoms ($Fe_2MnSi_{0.5}Ge_{0.5}$) cause to increase the electrical conductivity to its maximum value of about $1.1\times10^{20}(\Omega ms)^{-1}$ at 100 K and $1.4\times10^{20}(\Omega ms)^{-1}$ at 800 K. Further increasing in the content of Si atom ($Fe_2MnSi_{0.75}Ge_{0.25}$) led to reduce the electrical conductivity to be $0.9\times10^{20}(\Omega ms)^{-1}$ at 100 K and $1.3\times10^{20}(\Omega ms)^{-1}$ at 800 K. From above we can conclude that the increase/reduce in the electrical conductivity of $Fe_2MnSi_xGe_{1-x}$ alloys is attributed to the density of charge carriers (n) and their mobility ($\mu = e\tau/m_e$), since the electrical conductivity ($\sigma = ne\mu$) is related to the density of charge carriers and their mobility.

The Seebeck coefficient $S_{\alpha\beta}$ and the electrical conductivity $\sigma_{\alpha\beta}$ tensors can be written [47,49];

$$S_{\alpha\beta}(T;\mu) = \frac{1}{eT\Omega\sigma_{\alpha\beta}(T;\mu)}\int \sigma_{\alpha\beta}(\varepsilon)(\varepsilon-\mu)\times\left[-\frac{\partial f_\mu(T;\varepsilon)}{\partial\varepsilon}\right]d\varepsilon$$

$$\sigma_{\alpha\beta}(T;\mu) = \frac{1}{\Omega}\int \sigma_{\alpha\beta}(\varepsilon)\left[-\frac{\partial f_\mu(T;\varepsilon)}{\partial\varepsilon}\right]d\varepsilon$$

From above formulas it is clear that the Seebeck coefficient is inversely proportional to the electrical conductivity, and these quantities are functions of temperature (T) and chemical potential (μ) [47,49].

Fig. 3b illustrated the Seebeck coefficient (S) as a function of temperature at certain value of chemical potential (μ). Following Fig.3b one can see that the S for Fe_2MnGe is negative over the entire temperature range, which represents the n-type concentration. It is clear that S reduces rapidly with increasing the temperature, it posses the maximum value at 100 K (-0.2×10^{-5} $\mu V/K$) and the lowest value at 800 K. Whereas Fe_2MnSi show positive S up to 250 K then drop to negative values, which confirm the existence of the p-type concentration between 100-250 K. When we substitute 0.25 of Ge atoms by Si ($Fe_2MnSi_{0.25}Ge_{0.75}$) we noticed that the Seebeck coefficient show the maximum positive value at 100 K (0.9×10^{-5} $\mu V/K$), then reduces with increasing the temperature till 270 K. Above this temperature S drop to negative values to reach lower value of about (-0.7×10^{-5} $\mu V/K$) at 800 K.

With substituting the half content of Ge atoms by the same content from Si atoms ($Fe_2MnSi_{0.5}Ge_{0.5}$) we noticed that the Seebeck coefficient reduced to show the maximum value at 100 K of about (0.2×10^{-5} $\mu V/K$) and drops to negative values at 230 K to reach -0.8×10^{-5} $\mu V/K$ at 800 K. Further increasing the Si content on cost of Ge content ($Fe_2MnSi_{0.75}Ge_{0.25}$) the value of Seebeck coefficient at 100 K increases to be 0.6×10^{-5} $\mu V/K$ with respect to the value of S obtained for $Fe_2MnSi_{0.5}Ge_{0.5}$, then drops to negative values at 320 K.

Fig.3c show the electronic power factor ($S^2\sigma$) verses the temperature at certain value of chemical potential (μ) and constant relaxation time τ. We notice that the power factor of Fe_2MnGe rapidly increases with increasing the temperature to reach the maximum value (9×10^{10} $W/m\cdot K^2\cdot s$) at 800 K. While for Fe_2MnSi the power factor is zero till 300 K then rapidly increases with increasing the temperature to reach the maximum value (3.9×10^{10} $W/m\cdot K^2\cdot s$) at 800 K. With replacing 0.25 of Ge atoms by Si ($Fe_2MnSi_{0.25}Ge_{0.75}$) the power factor increases with respect to all other concentration to show its maximum value of about (0.8×10^{10} $W/m\cdot K^2\cdot s$) at 100 K, then reduces with increasing the temperature to reach zero value of $S^2\sigma$ between 250-350 K. Above this temperature range the $S^2\sigma$ increases with increasing the temperature to reach 0.2×10^{10} $W/m\cdot K^2\cdot s$ at 800 K. Substituting 0.5 of Ge atoms by Si ($Fe_2MnSi_{0.5}Ge_{0.5}$) cause to drop the value of power factor to zero up to 320 K. Then above 350 K the power factor increases with increasing the temperature to reach 1.0×10^{10} $W/m\cdot K^2\cdot s$ at 800 K. In the last case ($Fe_2MnSi_{0.75}Ge_{0.25}$) when we reduced the content of Ge to be 0.25 the power factor become $0.4\times10^{10}\ W/m\cdot K^2\cdot s$ at 100 K then drop to be zero between 200-500 K, above 500 K the Seebeck coefficient show an insignificant increasing to reach 0.2×10^{10} $W/m\cdot K^2\cdot s$ at 800 K.

The electronic thermal conductivity (κ_e) can be estimated from the electrical conductivity σ using Wiedemann-Franz law. Fig.3d, illustrated κ_e for $Fe_2MnSi_xGe_{1-x}$ alloys as a function of temperature at certain value of chemical potential. We notice that for all $Fe_2MnSi_xGe_{1-x}$ alloys κ_e increases rapidly with increasing the temperature. The end compound Fe_2MnSi show the highest value of κ_e between 100-800 K. While κ_e for Fe_2MnGe lie directly below that of Fe_2MnSi exhibiting the same trend. When we replace quarter of Ge atoms by Si ($Fe_2MnSi_{0.25}Ge_{0.75}$) the thermal conductivity drop down to show the lowest value along the temperature scale. With increasing the content of Si atoms to be equal to that of Ge atoms ($Fe_2MnSi_{0.5}Ge_{0.5}$) one can see that the κ_e values increases along the temperature scale. Substituting more Ge atoms by Si atoms ($Fe_2MnSi_{0.75}Ge_{0.25}$) led to reduce the values of the electronic thermal conductivity with respect to that of $Fe_2MnSi_{0.5}Ge_{0.5}$. Following Fig. 3d one can conclude that the electronic thermal conductivity is very sensitive to the density of charge carriers and their mobility. The thermal conductivity has contributions from the lattice and electrons. BoltzTraP calculates only the electronic part. In the absence of any calculations or measurements of the lattice thermal conductivity it is difficult to which alloy will have the largest figure of merit (FOM).

The electronic heat capacity $c_{el}(T_{el})$ for $Fe_2MnSi_xGe_{1-x}$ alloys as function of temperature at certain value of chemical potential with constant relaxation time is plotted in Fig. 3e. Here, we consider only the electronic contribution to the specific heat, because there is a linear relationship between the electronic specific heat and temperature i.e. $c_{el}(T_{el})=\gamma T_{el}$, where $\gamma =$ Sommerfeld coefficient [50,51]. The electrons excited to upper empty space and also result smearing of Fermi below the Fermi level, which contribute to the heat capacity. From Fig. 3e, one can see that the heat capacity for the end compounds (Fe_2MnGe and Fe_2MnSi) slowly increases with temperature up to 500 K, then reach the saturation up to 800 K. The $Fe_2MnSi_{0.25}Ge_{0.75}$ alloy show higher values of $c_{el}(T_{el})$ in comparison to the parents. Increasing the Si content ($Fe_2MnSi_{0.5}Ge_{0.5}$) cause to reduce the $c_{el}(T_{el})$ lower than that of $Fe_2MnSi_{0.25}Ge_{0.75}$ and higher than that of the parents. Further increasing in the Si content ($Fe_2MnSi_{0.75}Ge_{0.25}$) cause to increase $c_{el}(T_{el})$ to show the highest value among the others. It is clear from Fig. 3e, that the electronic heat capacity of $Fe_2MnSi_xGe_{1-x}$ alloys obey Debye approximation (T^3), also called anharmonic approximation [52].

Fig.3f, presented the Hall coefficient R_H as a function of temperature, its value depends on the type, number, and properties of the charge carriers that constitute the current. It is clear that the parents compounds (Fe_2MnGe and Fe_2MnSi) show the highest positive value of R_H at 100 K then rapidly reduces with increasing the temperature to cross the zero line to reach the negative values at 260 K. Above 360 K the R_H for the parents compounds almost saturated. The R_H for $Fe_2MnSi_{0.25}Ge_{0.75}$, $Fe_2MnSi_{0.5}Ge_{0.5}$ and $Fe_2MnSi_{0.75}Ge_{0.25}$ alloys exhibits negative R_H along the temperature scale that is attributed to the concentration of the charge carrier and their mobility.

To the best of our knowledge, there are no previous experimental data or theoretical results for the thermoelectric properties of the investigated materials available in literature to make a meaningful comparison. We would like to mention here that in our previous works [53–59] we have calculated the band gap, bond lengths, bond angles, linear and nonlinear optical susceptibilities using FPLAPW method on several systems whose energy band gap, bond lengths, bond angles, the linear and nonlinear optical susceptibilities are known experimentally. We find very good agreement with the experimental data. Thus, we believe that our calculations reported in this paper would produce very accurate and reliable results. Which prove the accuracy of the method we used.

4. Conclusions

The full potential linear augmented plane wave plus local orbitals method as implemented in WIEN2k code with the Engel-Vosko generalized gradient approximation for the exchange correlation potential were used to calculated band structure for $Fe_2MnSi_xGe_{1-x}$ (x=0.0, 0.25, 0.5, 0.75 and 1.0) alloys. Based on the calculated band structure the semi-classical Boltzmann theory as implemented in the BoltzTraP code was used to study the influence of vary the germanium content on the thermoelectric properties of $Fe_2MnSi_xGe_{1-x}$ alloys as a function of temperature at certain value of chemical potential (μ) with constant relaxation time (τ). The increase/reduce in the electrical conductivity ($\sigma = ne\mu$) of $Fe_2MnSi_xGe_{1-x}$ alloys is attributed to the density of charge carriers (n) and their mobility ($\mu = e\tau/m_e$). The parent Fe_2MnGe compound exhibit negative S over the entire temperature range which confirm the existence of n-type carrier. While Fe_2MnSi show positive S up to 250 K then drop to negative values, to represent the p-type charge carrier between 100-250 K. The alloys $Fe_2MnSi_{0.25}Ge_{0.75}$ / $Fe_2MnSi_{0.5}Ge_{0.5}$ / $Fe_2MnSi_{0.75}Ge_{0.25}$ possess positive S till 270 / 230 /320 K. Above these temperatures the Seebeck coefficient exhibit negative values. The power factor of Fe_2MnGe rapidly increases with increasing the temperature, while for Fe_2MnSi it is zero till 300 K then rapidly increases with increasing the temperature. $Fe_2MnSi_{0.25}Ge_{0.75}$ have zero power factor between 250-350 K. While $Fe_2MnSi_{0.5}Ge_{0.5}$ show zero power factor up to 320 K. The $Fe_2MnSi_{0.75}Ge_{0.25}$ alloy show zero power factor between 200-500 K. The electronic thermal conductivity (κ_e) and the electronic heat capacity $c_{el}(T_{el})$ increases with increasing the temperature. The parents compounds show the highest positive value of R_H at 100 K then drop to the negative values at 260 K. The alloys $Fe_2MnSi_{0.25}Ge_{0.75}$, $Fe_2MnSi_{0.5}Ge_{0.5}$ and $Fe_2MnSi_{0.75}Ge_{0.25}$ alloys exhibits negative R_H along the temperature scale. The positive and negative behavior of R_H is attributed to the concentration of the charge carrier and their mobility.

Acknowledgment

The result was developed within the CENTEM project, reg. no. CZ.1.05/2.1.00/03.0088, co-funded by the ERDF as part of the Ministry of Education, Youth and Sports OP RDI program.

References

[1] K. E. H. M. Hanssen, P. E. Mijnarends, L. P. L. M. Rabou and K. H. J. Buschow, Phy. Rev. B42 (1990)1533.

[2] H. Kino, F. Aryasetiawanx, I. Solovyer, T. Miyake, T. Ohno and K. Terakura, Physica B 329 (2003)858.

[3] R. A. de Groot, Physica B 172 (1991)45.

[4] J. H. Wijngaard, C. haas, R. A. de Groot, Phy. Rev. B40 (1989) 9318.

[5] S. Chadov, J. Minar, H. Ebert, A. Perlov, L. Chioncel, M. I. Katsnelson and A. I. Lichtenstein, Phy. Rev. B74 (2006) 140411.

[6] B. I. Min, T. Oguchi, H. J. F. Jansen and A, J. Freeman, Phy. Rev. B33 (1986) 324.

[7] G. A. de Wijs and R. A. de Groot, Phy. Rev. B64 (2001) 020402.

[8] E. Kisker, C. carbone, C. F. Flipse and E. F. Wassermann, J. Magn. Magn. Mater.70 (1987) 21.

[9] I. Galanakis, P. H. Dederichs and N. Papanikolaou , Phy. Rev. B66 (2002) 174429.

[10] K. Nagao, M. Shirai and Y. Miura, J. Phys. :Condens. Matter 16, (2004) 5725.

[11] K. Schwarz, J. Phys. F: Met. Phys. 16 (1986) 211.

[12] I. I. Mazin, D. J. Singh and C. Ambrosch-Draxl, Phy. Rev. B59 (1999) 411.

[13] G. L. Zhao, J. Callaway and M. Hayashibara, Phy. Rev. B48 (1993) 15781.

[14] G. A. Prinz, Science 282(1998) 1660.

[15] S. A. Wolf, D. D. Awschalom, R. A. Buhrman, J. M. Daughton, S. von Molnar, M. L. Roukes, A.Y. Chtchelkanova, D. M. Treger, Science 294(2001) 1488.

[16] I. Zutic, J. Fabian, S. Das Sarma, RMP 76 (2004) 323.

[17] D. D. Awschalom, M. E. Flatte, Nat Phys 3(2007) 153.

[18] T. Akimoto, Y. Moritomo, A. Nakamura and N. Furukawa, Phys. Rev. Lett. 85 (2000) 3914.

[19] C. M. Fang, G. A. de Wijs and R. A. de Groot, J. Appl. Phys. 91 (2002) 8340.

[20] H. Ohno, Science 281 (1998) 951.

[21] S. J. Pearton,C. R. Abernathy, M. E. Overberg, G.T.Thaler, D. P. Norton, N.Theodoropoulou, A. F. Hebard, Y. D. Park, F. Ren, J. Kim and L. A. Boatner,J. Appl. Phys. 93 (2003)1.

[22] A. M. Goldman, V. Vasko, P. Kraus, K. Nikolaev and V. A. Larkin ,J. Mag. Magn. Mater. 200 (1999) 69.

[23] V. Dediu, M. Murgia, F. C. Matacotta, C. Taliani and S. barbanera, Solid state Commun. 122 (2002)181

[24] A. J. Epstein, MRS Bull. 28 (2003) 492.

[25] D. A. Pejakovic, C. Kitamura, J. S. Miller and A. J. Epstein, Phys. Rev. Lett. 88 (2002) 057202.

[26] B. Zhao, I. Monch, H. Vinzelberg, T. Muhl and C. M. Schneider, Appl. Phys. Lett. 80 (2002) 3144.

[27] K. Tsukagoshi, B. W. Alphenaar and H. Ago, Nature 401 (1999) 572.

[28] R. A. de Groot, F. M. Mueller, P. G. van Engen and K. H. J. Buschow, Phys. Rev. Lett. 50 (1983) 2024.

[29] R. A. de Groot, F. M. Mueller, P. G. van Engen and K. H. J. Buschow, J. Appl. Phys. 55 (1984) 2151.

[30] J. W. Dong, L. C. Chen, J. C. Palmstom, R. D. James and S. Mckernan, Appl . Phys. Lett .75 (1999)1443.

[31] S. M. Watta, S. Wirth, S. Von Molnar, A. Barry and J. M. D. Coey, Phy. Rev. B61 (2000) 9621.

[32] F. J. Jedema, A. T. Filip, B. van Wees, Nature 410 (2001) 345.

[33] J. Kubler, Physica B 127 (1984) 257.

[34] K. E. H. M. Hanssen and P. E. Mijnarends, Phy. Rev. B34 (1986) 5009.

[35] I. Galanakis, S. Ostanin, M. Alouani, H. Dreysse and J. M. Wills, Phys. Rev. B 61(2000)4093.

[36] B. G. Liu, Phys. Rev. B67 (2003) 172411.

[37] I. Galanakis, Phys. Rev. B66 (2002) 012406.

[38] S. P. Lewis, P. B. Allen and T. Sasaki, Phys. Rev. B55 (1997) 10253.

[39] R. A. de Groot and K. H. J. Buschow, J. Mag. Magn. Mater. 54 (1986) 1377.

[40] I. Galanakis, J. Phys.: Condens. Matter 14 (2002) 6329.

[41] S. Fujii, S.Ishida, and S. Asano, J. Phys. Soc. Jpn. **64** (1995).

[42] L. Hongzhi, Z. Zhiyong, M. Li, X. Shifeng, L. Heyan, Q. Jingping, L. Yangxian and W. Guangheng, J. Phys. D: Appl. Phys. 40 (2007) 7121.

[43] B. Hamad, J. Khalifeh, I. Adu Aljarayesh, C. Demangeat, H-B Luo and Q-M Hu, J. Appl. Phys. 107 (2010) 09311.

[44] K. Ueda, K. Hamaya, K. Yamamoto, Y. Ando, T. Sadoh, Y. Maeda, and M. Miyao, Appl. Phys. Lett. **93** (2008) 112108.

[45] l. Zhang, E. Bruck, O. Tegus, H. H. J. Buschow, F.R. de Boer, Physica B 328 (2003) 295.

[46] Georg K. H. Madsen, David J. Singh, cond-mat.mtrl-sci. 8 Feb 2006

[47] Madsen G K H and Singh D J 2006 *Comput. Phys. Commun.* **175** 67-71

[48] P. Blaha, K. Schwarz, G. Madsen, D. Kvasnika and K. Luitz, WIEN2k, Technical Universität Wien, Austria, 2001; ISBN 3-9501031-1-2.

[49] Hua P, Lei W C, Chao L J, Rui-Zhi Z, Hong-Chao W, and Chin S Y 2011 *Phys. B* 20(4) 046103

[50] N. W. Ashcroft and N. D. Mermin, Solid State Physics (Holt, Rinehart and Winston, New York, 1976)

[51] Z. Zhang, Nano/Microscale Heat Transfer, McGraw-Hill, New York, 2007.

[52] Chen Dong et al. Chinese Physics B 1674-1056/2009/18(02)/0738-06.

[53] A. H. Reshak, S. Auluck, and I. V. Kityk, J. Phys.: Condens. Matter 20, 145209 (2008).

[54] A. H. Reshak, S. Auluck, and I. V. Kityk, J. Solid State Chem. 181, 789–795 (2008).

[55] A. H. Reshak, J. Chem. Phys. 124, 104707 (2006).

[56] A. H. Reshak, Eur. Phys. J. B 47, 503–508 (2005).

[57] A. H. Reshak, I. V. Kityk, and S. Auluck, J. Phys. Chem. B 114, 16705–16712 (2010).

[58] A. H. Reshak, S. Auluck, D. Stys, I. V. Kityk, H. Kamarudin, J. Berdowski, and Z. Tylczynskif, J. Mater. Chem. 21, 17219 (2011).

[59] A. H. Reshak,M. Piasecki, S. Auluck, I. V. Kityk, R. Khenata, B. Andriyevsky, C. Cobet, N. Esser, A. Majchrowski, M. S'wirkowicz, R. Diduszko, and W. Szyrski, J. Phys. Chem. B 113(46), 15237 (2009).

Table I: The density of states at Fermi energy $N(E_F)$ states/eV cell and the bare electronic specific heat coefficient γ (mJ/mole-K^2) of $Fe_2MnSi_xGe_{1-x}$ (x=0.0, 0.25, 0.5, 0.75, 1.0) alloys.

	Fe_2MnGe	**$Fe_2MnSi_{0.25}Ge_{0.75}$**	**$Fe_2MnSi_{0.5}Ge_{0.5}$**	**$Fe_2MnSi_{0.75}Ge_{0.25}$**	**Fe_2MnSi**
$N(E_F)$states/eV cell	17.11	65.0	33.93	58.15	16.07
γ (mJ/mole-K^2)	2.96	11.27	5.88	10.08	2.78

Figure captions

Fig. 1: The structure of the unit cell of $Fe_2MnSi_xGe_{1-x}$ (x=0.0, 0.25, 0.5, 0.75 and 1.0) alloys.

Fig. 2: (a-e) Calculated electronic band structure of $Fe_2MnSi_xGe_{1-x}$ (x=0.0, 0.25, 0.5, 0.75 and 1.0) alloys.

Fig. 3: (a) Calculated electrical conductivity; (b) Calculated Seebeck coefficient; (c) Calculated power factor; (d) Calculated electronic thermal conductivity; (e) Calculated electronic heat capacity; (f) Calculated Hall coefficient.

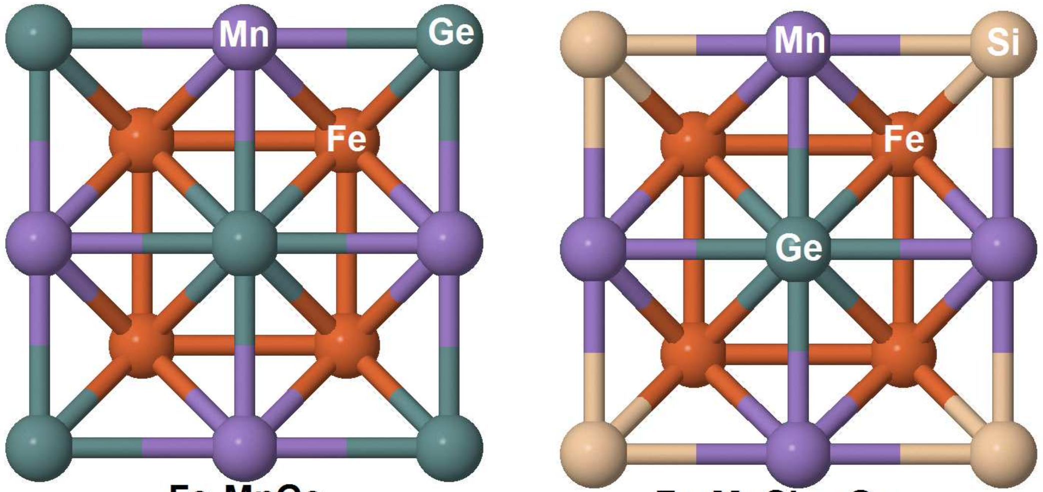

Fe_2MnGe $Fe_2MnSi_{0.25}Ge_{0.75}$

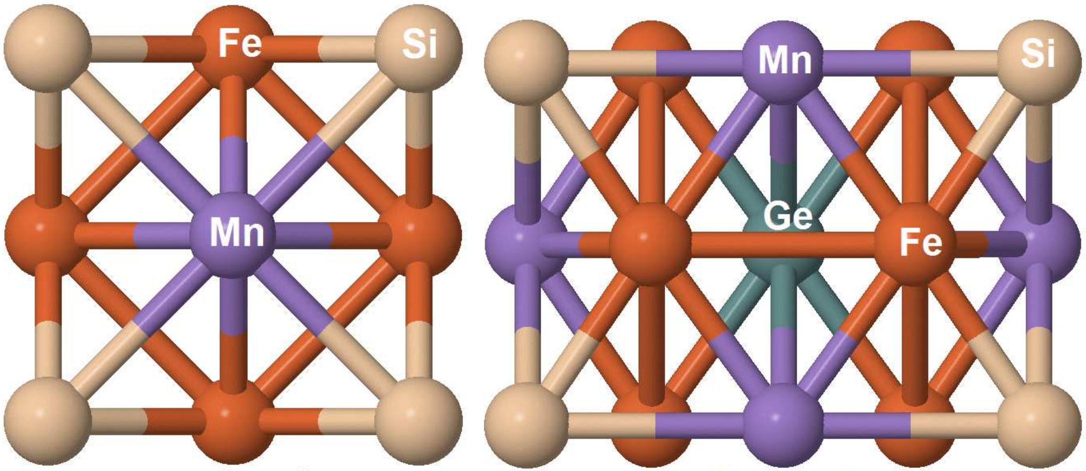

$Fe_2MnSi_{0.5}Ge_{0.5}$ $Fe_2MnSi_{0.5}Ge_{0.5}$

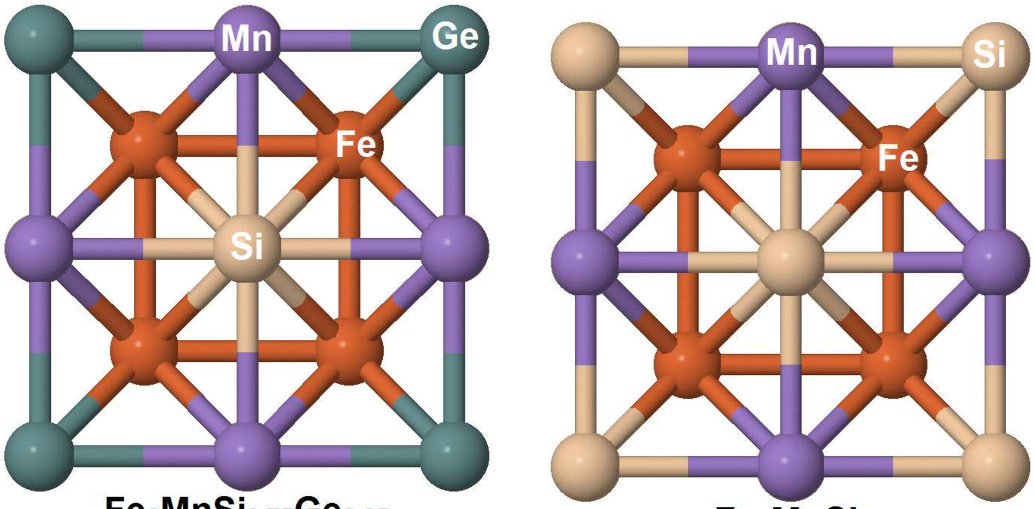

$Fe_2MnSi_{0.75}Ge_{0.25}$ Fe_2MnSi

Fig.1:

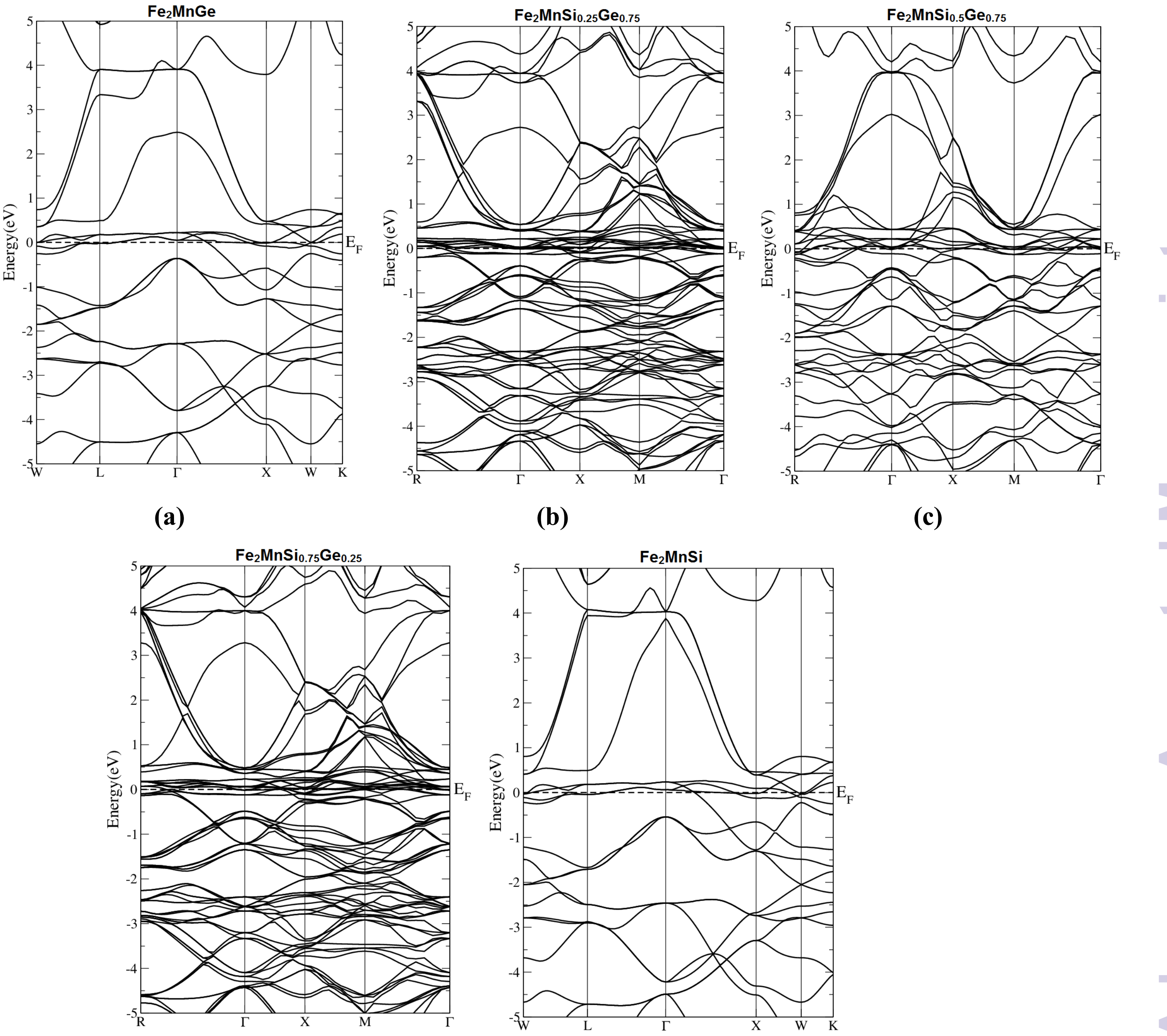
Fe_2MnGe
$Fe_2MnSi_{0.25}Ge_{0.75}$
$Fe_2MnSi_{0.5}Ge_{0.75}$
$Fe_2MnSi_{0.75}Ge_{0.25}$
Fe_2MnSi
Energy(eV)
E_F
W
L
Γ
X
W
K
R
Γ
X
M
Γ
5
4
3
2
1
0
-1
-2
-3
-4
-5

(a) (b) (c)

(d) (e)

Fig.2:

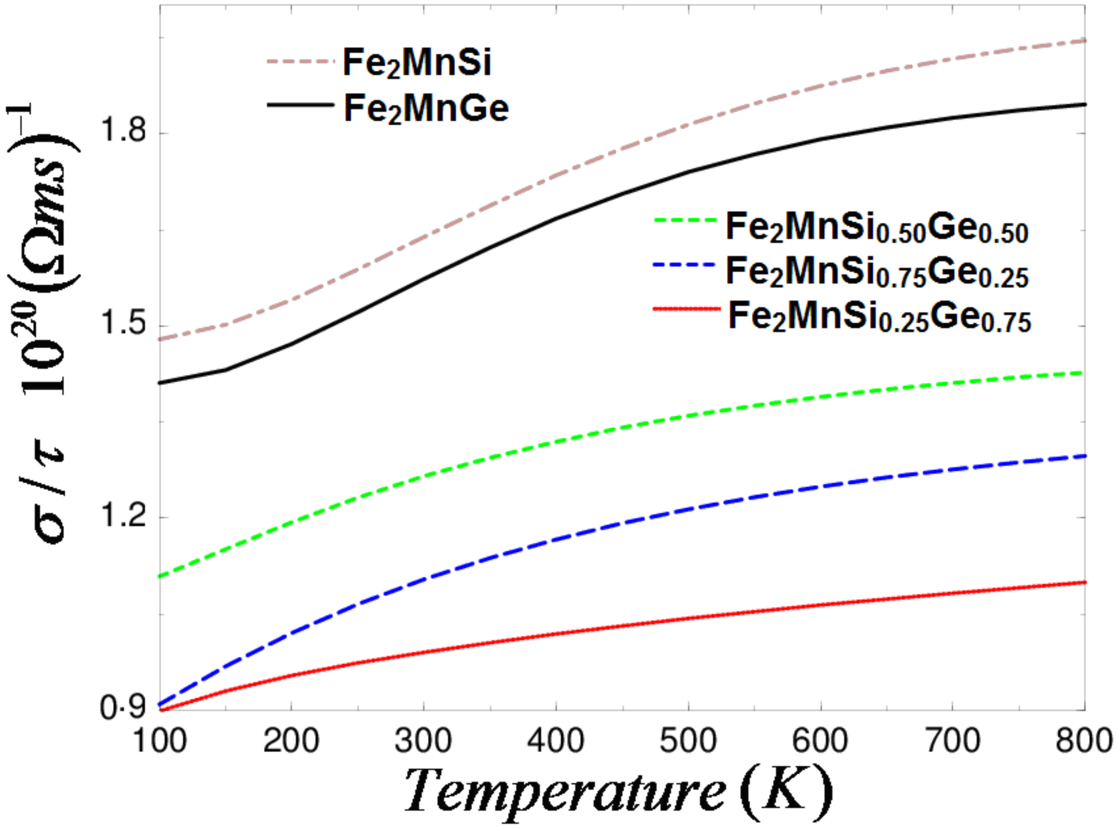
Fe2MnSi
Fe2MnGe
Fe2MnSi0.50Ge0.50
Fe2MnSi0.75Ge0.25
Fe2MnSi0.25Ge0.75
σ / τ 10^20 (Ωms)^-1
1.8
1.5
1.2
0·9
100
200
300
400
500
600
700
800
Temperature (K)

(a)

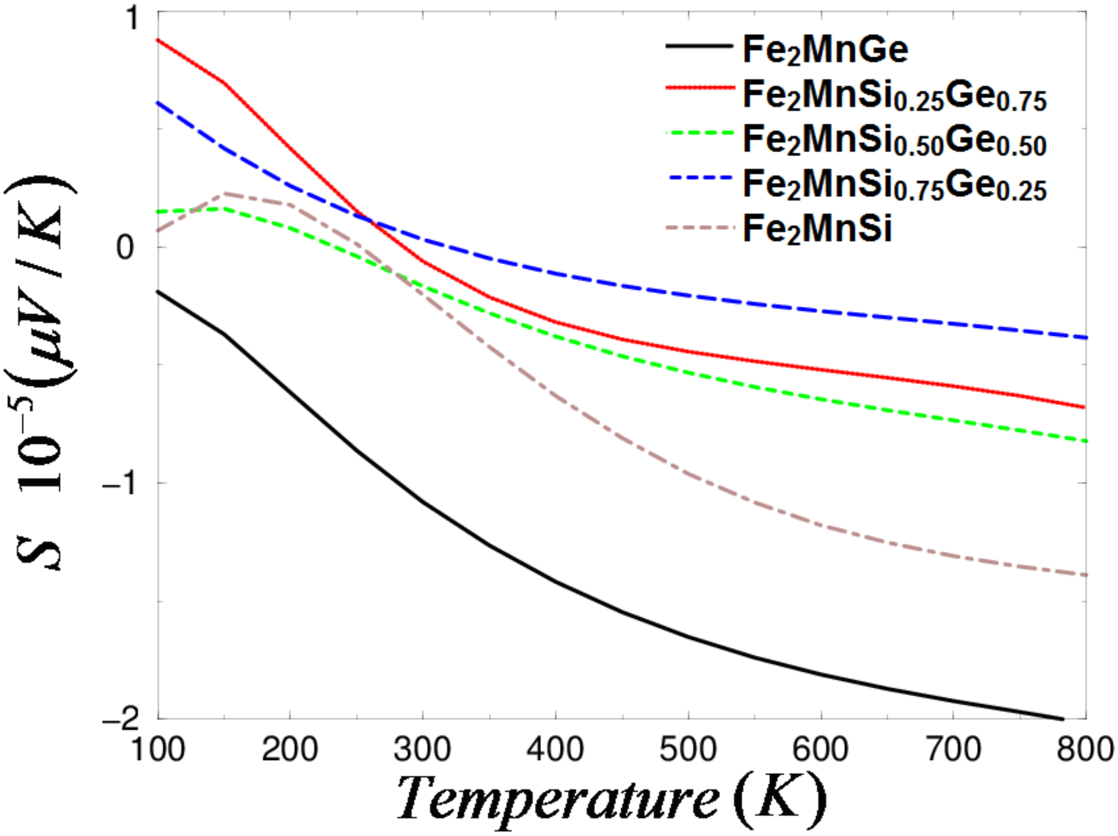
Fe₂MnGe
Fe₂MnSi0.25Ge0.75
Fe₂MnSi0.50Ge0.50
Fe₂MnSi0.75Ge0.25
Fe₂MnSi
S 10⁻⁵(μV / K)
Temperature (K)
1
0
−1
−2
100
200
300
400
500
600
700
800

(b)

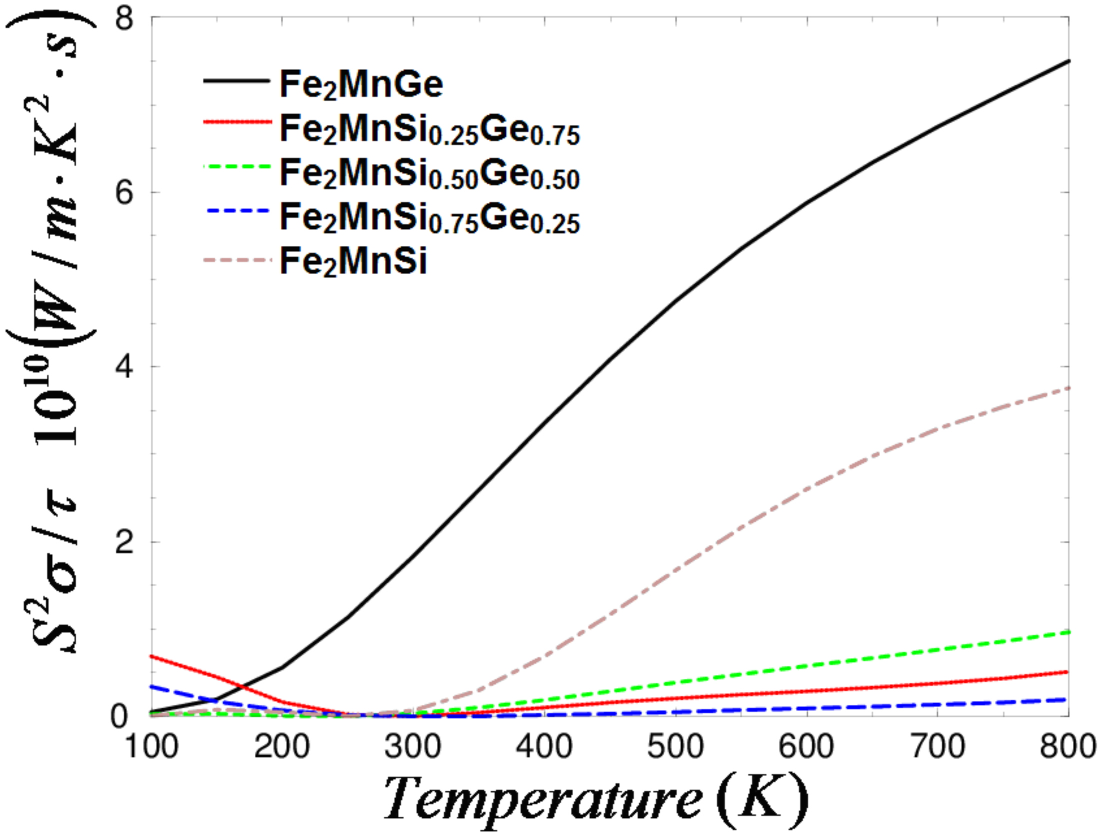
$S^2\sigma/\tau$ $10^{10}(W/m\cdot K^2\cdot s)$
8
6
4
2
0
100
200
300
400
500
600
700
800
$Temperature\ (K)$
Fe_2MnGe
$Fe_2MnSi_{0.25}Ge_{0.75}$
$Fe_2MnSi_{0.50}Ge_{0.50}$
$Fe_2MnSi_{0.75}Ge_{0.25}$
Fe_2MnSi

(c)

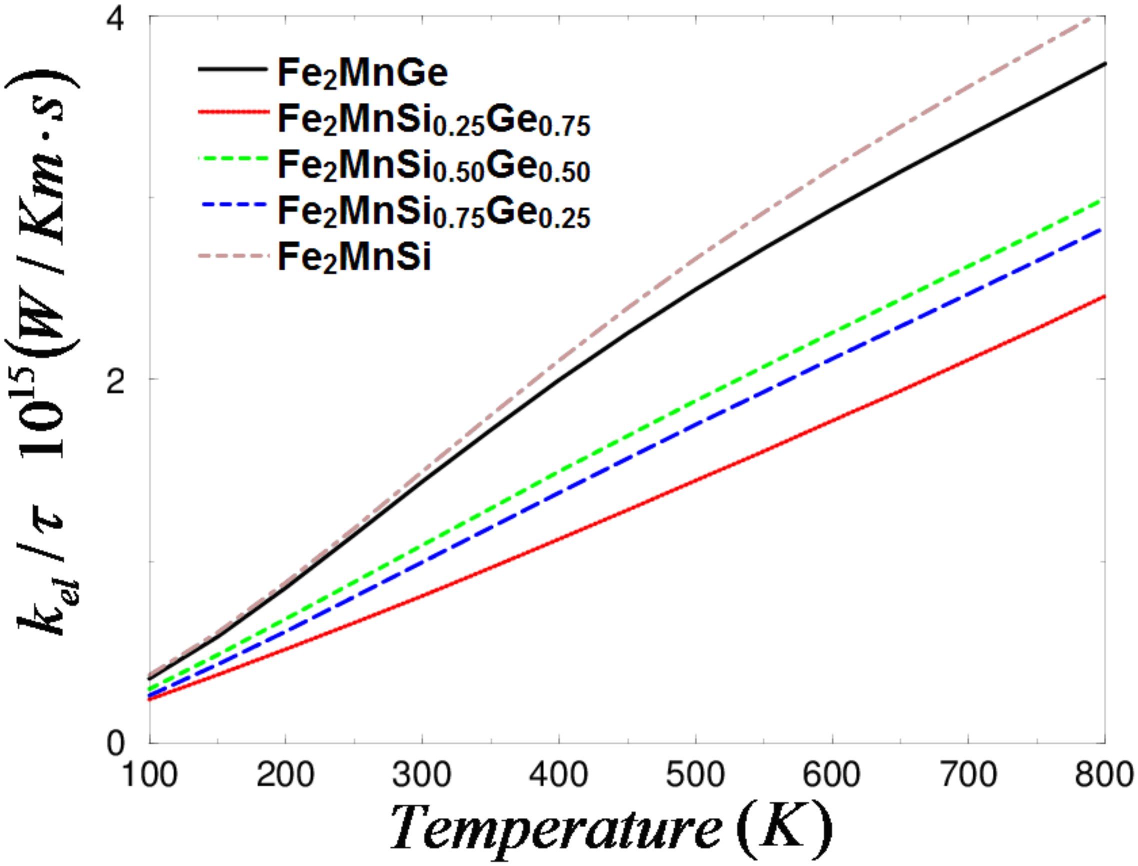

4
2
0
$k_{el}/\tau\ \ 10^{15}(W/Km\cdot s)$
Fe2MnGe
Fe2MnSi0.25Ge0.75
Fe2MnSi0.50Ge0.50
Fe2MnSi0.75Ge0.25
Fe2MnSi
100
200
300
400
500
600
700
800
Temperature (K)

(d)

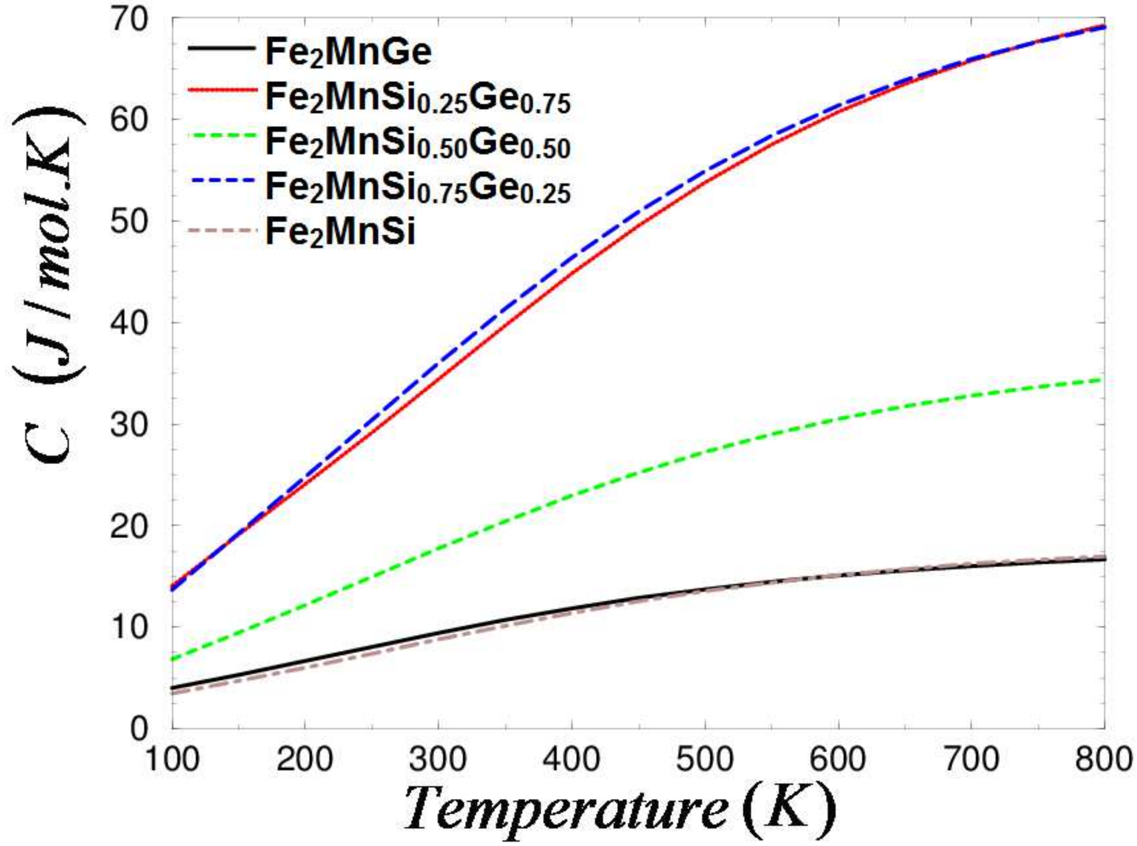
Fe2MnGe
Fe2MnSi0.25Ge0.75
Fe2MnSi0.50Ge0.50
Fe2MnSi0.75Ge0.25
Fe2MnSi
C (J/mol.K)
Temperature (K)
0
10
20
30
40
50
60
70
100
200
300
400
500
600
700
800

(e)

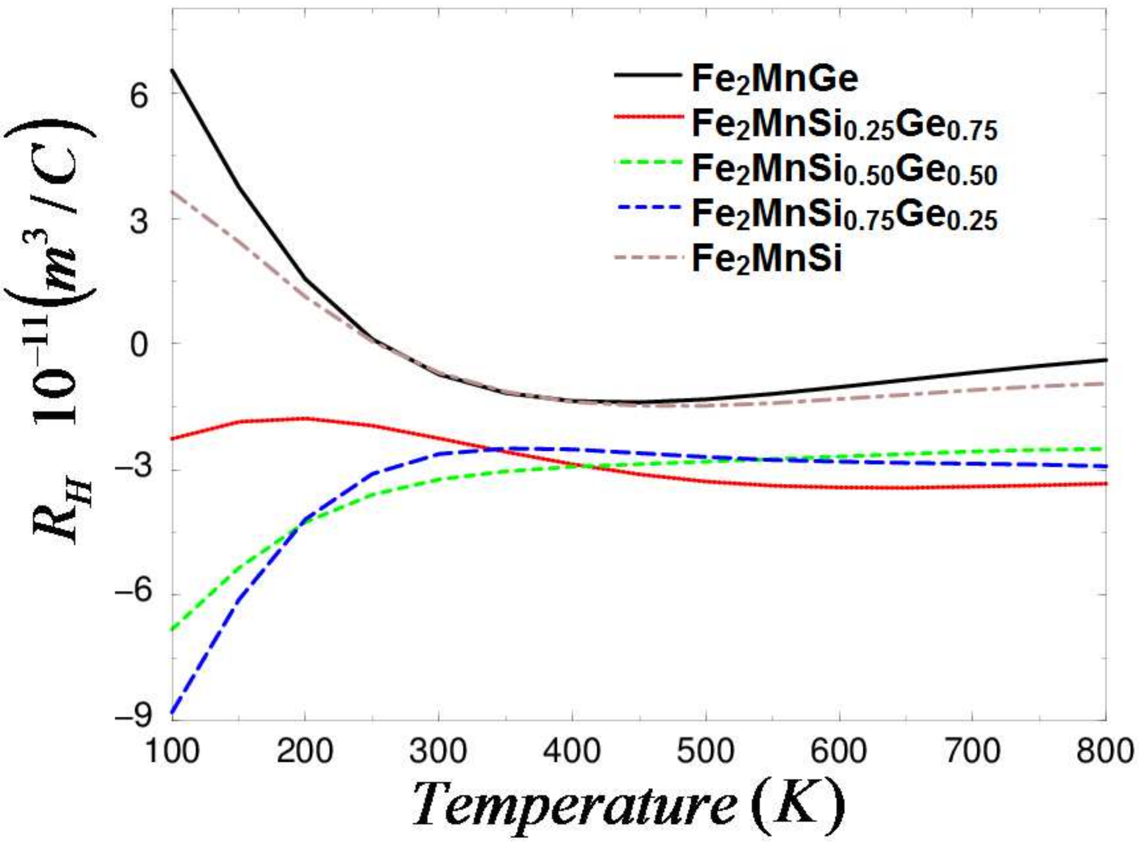
Fe2MnGe
Fe2MnSi0.25Ge0.75
Fe2MnSi0.50Ge0.50
Fe2MnSi0.75Ge0.25
Fe2MnSi
$R_H \quad 10^{-11}(m^3/C)$
6
3
0
−3
−6
−9
100
200
300
400
500
600
700
800
Temperature (K)

(f)

Fig.3: